IYNC 2008
Interlaken, Switzerland, 20 – 26 September 2008
Paper No. 163

Simulating the Behaviour of the Fast Reactor JOYO

Pauli Juutilainen
VTT Technical Research Centre of Finland, P.O. Box 1000, 02044 VTT, Finland
pauli.juutilainen@vtt.fi

ABSTRACT

Motivated by the development of fast reactors the behaviour of the Japanese experimental fast reactor JOYO was simulated with two Monte Carlo codes: Monte Carlo N-Particle (MCNP) and Probabilistic Scattering Game (PSG). The simulations were based on the benchmark study "Japan's Experimental Fast Reactor JOYO MK-I core: Sodium-Cooled Uranium-Plutonium Mixed Oxide Fueled Fast Core Surrounded by UO2 Blanket". The study was focused on the criticality of the reactor, control rod worth, sodium void reactivity and isothermal temperature coefficient of the reactor. These features were calculated by applying both homogeneous and heterogeneous reactor core models that were built according to the benchmark instructions. The results of the two models obtained by the two codes were compared to each other and to the experimental results presented in the benchmark. The codes yielded quite similar results, but it also became obvious that Monte Carlo method does not suit very well in reactor scale simulations, especially when small changes of the multiplication factor are considered.

1 INTRODUCTION

If any uranium-based nuclear power is going to be deployed also in the remote future, the introduction of reactors with fast neutron spectrum will be necessary. Therefore, almost all major industrial countries have contributed to the fast breeder reactor (FBR) development over the decades since the beginning of the nuclear era. The high costs, technological difficulties and public resistance accompanied by nuclear proliferation concerns have caused some of the countries to bury their FBR programs. To some extent, the target of the efforts has shifted from the plan of producing energy to transmuting the spent fuel, also known as nuclear waste, to less harmful form. However, the fast breeder reactors would provide a method to generate large amounts of electricity, if the technology was developed to an adequate level to tackle the problems previously listed.

One of the nations still aiming at producing energy by fast reactors is Japan, whose FBR program has been motivated by the scarcity of domestic energy resources. The experimental fast breeder reactor JOYO has operated as a part of the Japanese fast reactor development program since 1977. The experiments referred to in the present study were completed in the beginning of the operation, originally without any significant intentions to create an ideal benchmark. However, the results and measurement conditions of the series of experiments have been later determined to be sufficient to allow the use of them as a benchmark [1]. For the present study it signifies that the results can be used for verification of computer simulation codes by simulating the experiments and comparing the experimental and computational results. The codes employed here are the Monte Carlo codes MCNP (version 4C) and PSG. It is observed that in some cases the characteristics of the reactor may be estimated quite accurately, but also that the suitability of the Monte Carlo method encounters certain limits.

2 COMPUTATIONAL METHODS

Traditionally the life of the neutrons in reactor has been calculated by employing deterministic transport codes. Following the continuous improvements of computational power and algorithms the use of Monte Carlo simulation codes has become increasingly suitable option in reactor physics modelling, although the dominance of deterministic codes probably continues a long time. The deterministic codes are based on the procedure to solve valid neutron transport equations by using discretised values of the variables that are usually the space and momentum of the particles. All particles between two discretisation nodes thus have the same characteristics. In Monte Carlo method, for its part, every particle is treated as an individual, whose movements, reactions and lifetimes are determined by sampling such that the laws of physics and experimentally obtained statistical distributions are obeyed.

MCNP has been developed over its long history to serve as a general-purpose particle transport code. In addition to reactor criticality calculations it can be used to several kinds of applications related to nuclear technology. The particles to simulate may be photons, electrons and neutrons or they all together in the same system. In this work only neutrons were handled. The other code deployed in this work was PSG that has been developed at VTT Technical Research Centre of Finland for a little less than four years and can thus be regarded as a newcomer in the family of Monte Carlo codes. PSG has been intended to become a tool specified for reactor physics calculations, especially at the fuel bundle level. The main purpose of the code is to generate homogenized group constants for deterministic reactor simulator codes. Another goal in the development has been to create burn-up calculation that is a necessary feature when producing group constant data for irradiated fuel. [2]

PSG runs much faster than MCNP, which has been achieved by using a different internal data format concerning the treatment of the cross-section data. MCNP – as well as probably all the other Monte Carlo codes developed so far – uses separated energy grids for every nuclide and therefore the code has to search the right cross-section as a function of particle energy for all nuclides. PSG instead combines all energy grids to a large single grid so that the required cross-sections related to certain particle energy are gained for all nuclides with one grid search. The described approach reduces calculation time considerably. The price of this data processing shortcut is the increased need for memory, where the “mother of all grids” is saved over the simulation. This kind of wasteful memory usage has become possible to perform even with standard modern computers, especially for fresh fuel calculations. The situation may become more difficult when performing calculations with irradiated fuel that includes hundreds of various nuclides. Then the master grid grows significantly, but the growth can be hindered by removing data points that lie sufficiently close to each other. [2]

Another way utilized in PSG to speed up the calculation is the use of the Woodcock delta-tracking method in neutron tracking. It allows a simpler treatment of the geometry when the particle moves from a material to another. The movement is not needed to stop at the border for recalculation, because the same total cross-section is applied in every material. The method limits the simulation generality such that it works poorly for example in detector modelling. Therefore it has not been used in general-purpose Monte Carlo codes, but for reactor physical means it suits well enough. Further details concerning the Woodcock method are not represented here.

Both MCNP and PSG read the required cross-section data from ACE format libraries. By using the same data format one of the potential error sources is eliminated, which makes the comparison of the simulations performed by these codes easier. In the following simulations the library ENDF/B-VI was used.

3 THE JOYO REACTOR

The sodium-cooled experimental fast reactor JOYO achieved its first criticality in 1977. The core model used over the first operational years was called MK-I. The power was produced in the core fuel region that was surrounded by blanket fuel region. The core was fuelled by mixed-oxide (MOX) fuel that consisted of 23% enriched uranium and plutonium that accounted for 17.7% of the weight of all metallic material. The plutonium content for its part included 80.4% fissile plutonium. The material in the blanket region consisted of depleted uranium including 0.2% fissile ^{235}U. The blanket region was

also known as the breeding zone as the breeding of fissionable ^{238}U to fissile ^{239}Pu occurred mostly there. The leakage of the neutrons that were not captured in the blanket fuel was tried to stop by reflectors, both removable and fixed. In the beginning of operation the maximum thermal power of the reactor was 50 MWt, but it was soon upgraded to 75 MWt. Since 2003 the plant has been operating with the maximum thermal power of 140 MWt subsequent to the upgrade to MK-III core.

The experiments of the study were mostly performed for 64- and 70-fuel-subassembly cores, but also an assembly with 65 fuel subassemblies was employed when measuring the isothermal temperature coefficient. The Figure 1 presents a core pattern of a 70-fuel-subassembly core. In various experiments the exact locations of some core and blanket fuel subassemblies at the border of the two regions were slightly altered, but no major modifications were conducted.

As illustrated by the Figure 1, the subassemblies comprised a hexagonal lattice. The pitch diameter of a hexagon at room temperature was 8.15 cm. More accurately, this was the distance between the midpoints of adjacent hexagons, but the wrapper tubes surrounding the fuel pins were narrower to enable coolant to flow between them. A core fuel subassembly included 91 fuel pins that were vertically divided in core and blanket fuel regions. The core fuel region was axially located in the middle of the pin surrounded by the blanket fuel regions both below and above. The upper and lower ends of the subassemblies were formed by 20 cm thick reflectors. A radial blanket fuel subassembly included 19 fuel pins that were homogeneously filled by depleted uranium from bottom to top. They were surrounded by axial reflectors similarly to the core fuel subassemblies. A horizontal cross-section of core and radial blanket fuel subassemblies generated by the plotter of PSG is depicted in Figure 2.

The reactor was regulated by six control rods two of which were classified as regulation rods and four as safety rods. They were located in the core fuel region as is illustrated in Fig. 1. The actual neutron absorber region included 7 absorber elements that consisted of boron carbide (B_4C), see Fig. 3. Axially the neutron absorber region of the rods extended from a little below the core fuel region to a little above it. The axial arrangement of various fuel, absorber and reflector regions in the reactor is depicted in Figure 4.

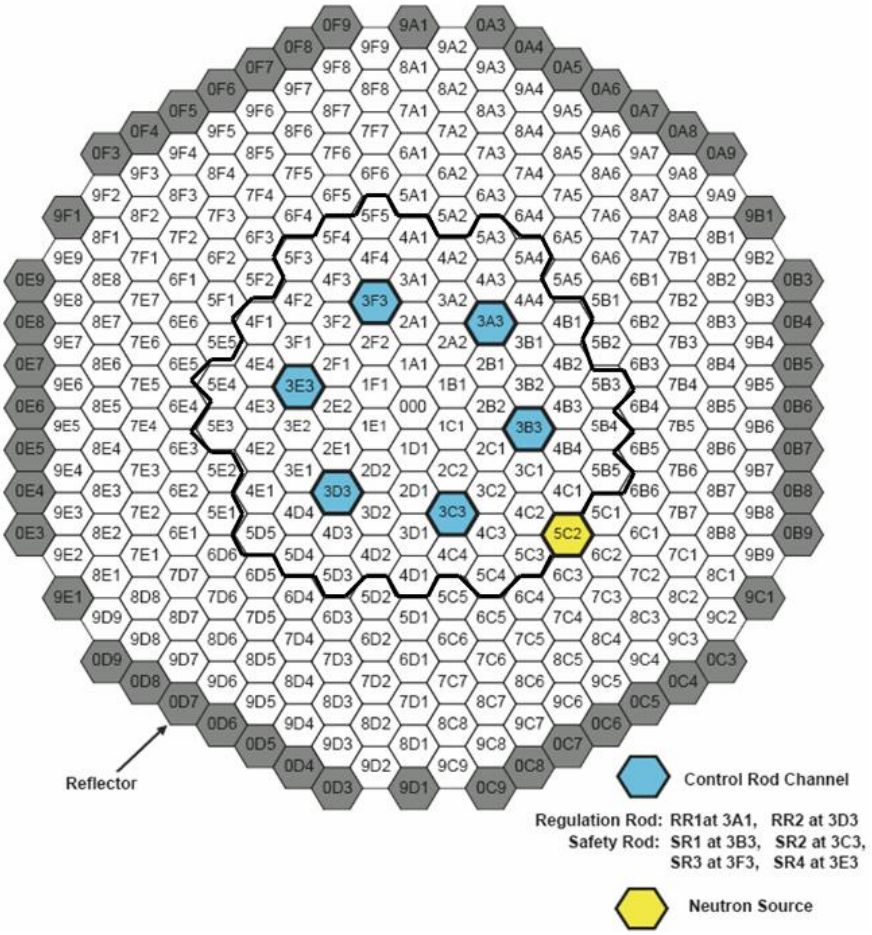

Figure 1: The horizontal cross-section of the 70-fuel-subassembly of Joyo. The core and blanket fuel regions are separated by the bold black line. This particular assembly was employed in sodium void reactivity measurements. In other measurements some of the core and blanket fuel subassemblies were organized slightly differently. [1]

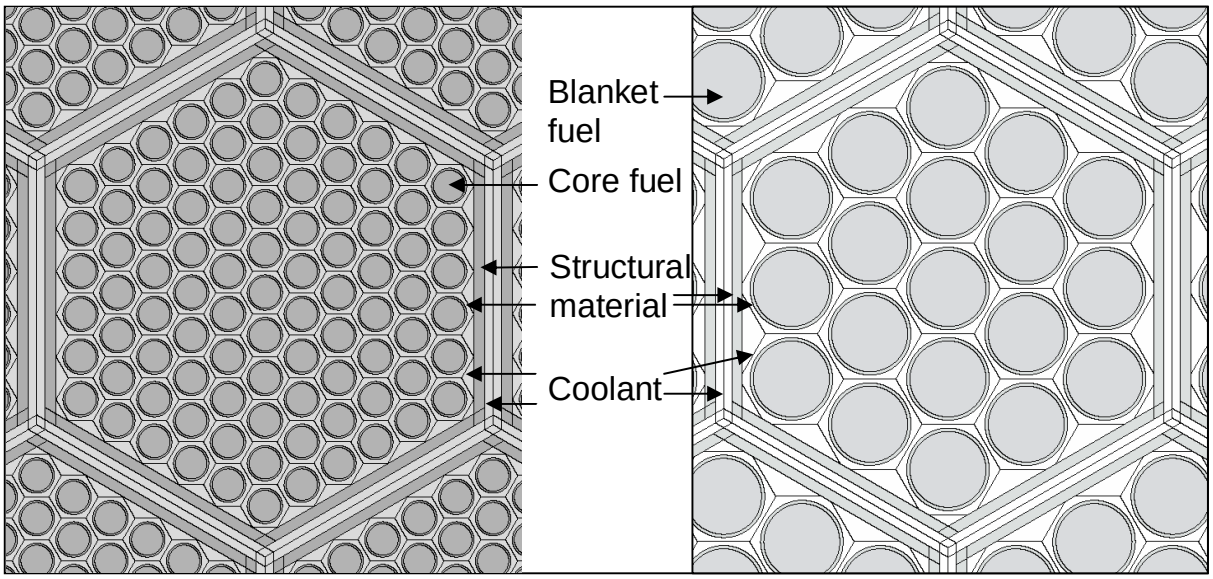

Figure 2: The contents of core (left) and blanket fuel subassemblies. Note that the lines forming hexagons between fuel pins and are only products of the plotter to illustrate the borders of the hexagonal lattice, they don't represent any physical surface.

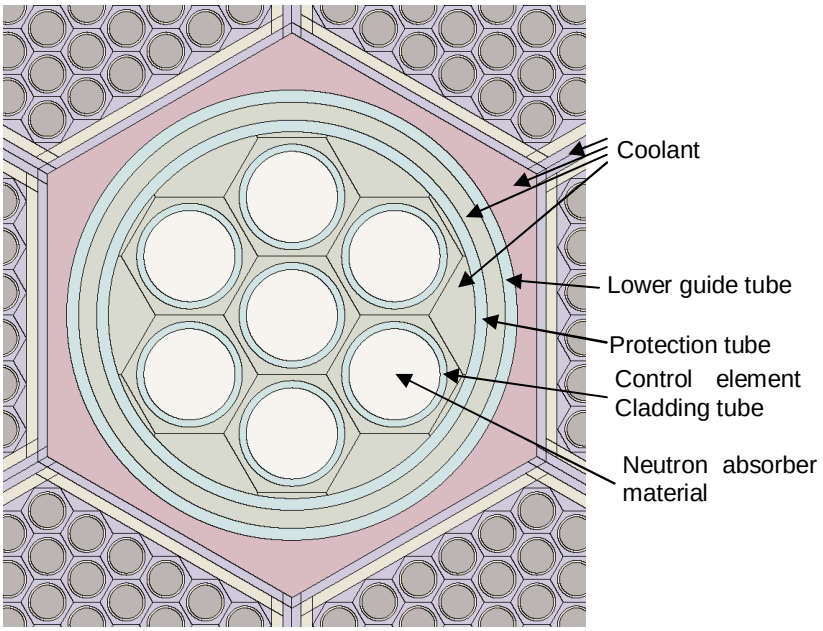

Figure 3: The neutron absorber region of a control rod subassembly. Again, the lines of the hexagons don't represent any physical surface, apart from those who form the wrapper tubes of the adjacent core fuel subassemblies.

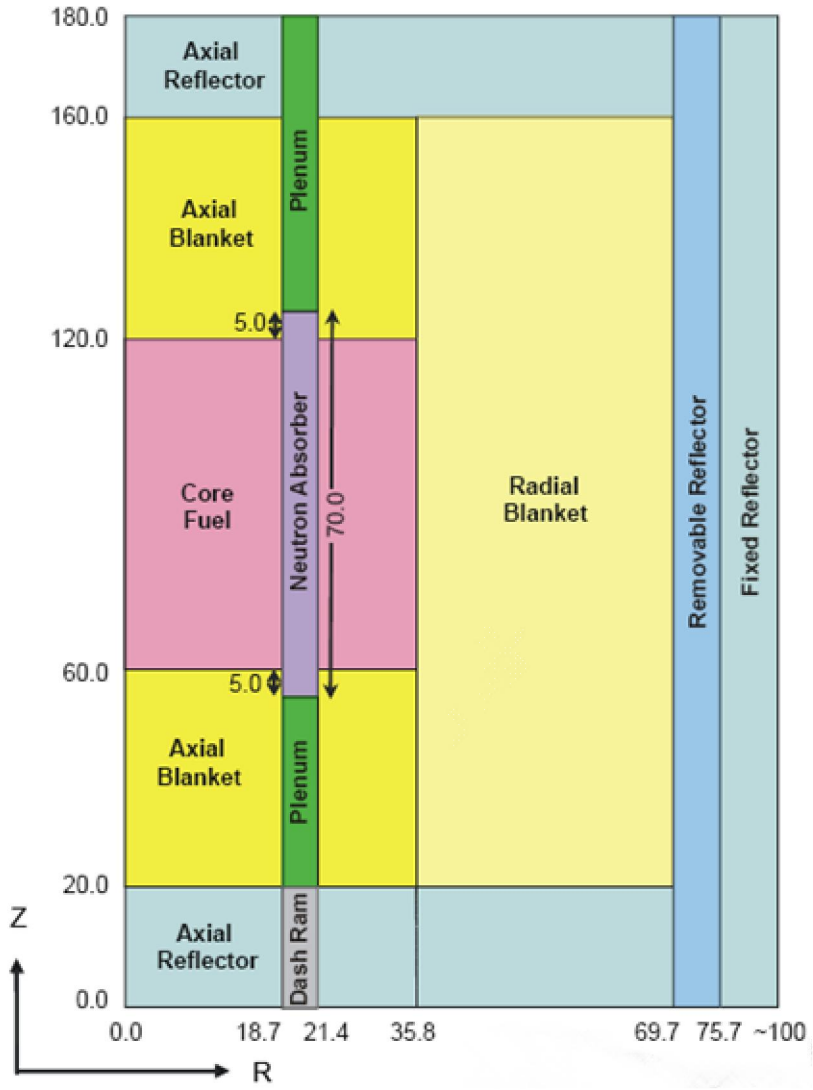

Figure 4: A rough vertical cross-section of JOYO. The control rod included in the picture is completely inserted. [1]

4 SIMULATIONS

4.1 Homogeneous and heterogeneous models

In homogeneous model the material included in a subassembly was supposed to be evenly mixed in the subassembly level. The accuracy of the modeling is what is presented in Fig. 1. Both the MCNP and PSG simulations were completed by 500 active calculation cycles preceded by 50 inactive ones with MCNP and 10 with PSG. The initial neutron population of 10 000 was used in all simulations with MCNP, while the PSG simulations used the population of 20 000 neutrons.

The heterogeneous model represented more detailed approach, since the core and blanket fuel subassemblies as well as the neutron absorber regions of the control rods were modeled as they appear in the real reactor. The details of the subassemblies are depicted in Figures 2 and 3. Other parts of the core were still handled as a homogeneous mix of materials at the accuracy of the subassembly level. The more detailed geometry description of course made the simulations

substantially slower, especially when MCNP was used. With PSG the calculation time increased much less. The neutron population for which the multiplication factor was calculated was kept at 20 000 in PSG simulations but increased to 15 000 in MCNP simulations. The neutron population of the MCNP simulations was increased, because the code warned for fissile cell elements in which no neutrons visited. The result might have been a smaller value of the multiplication factor. However, even with the increased population some this kind of cells still existed, but the effect is assumed to be negligible. The numbers of calculation cycles were kept at the same figures with the homogeneous model.

When examining the experimental results, it should be noted that they have been modified to be comparable with simulations. Consequently, the measured values presented in tables with the simulation results of the homogeneous model differ from those appearing in the tables with the heterogeneous model simulations. In the following subsections everything that refers to something experimental uses the benchmark of the JOYO-reactor [1] as the reference.

4.2 Criticality

The first criticality of JOYO was achieved by adding core fuel subassemblies one-by-one with all control and safety rods, except for RR2, fully withdrawn until the criticality was reached. The milestone was broken with 64 fuel subassemblies at the temperature of 204.7°C. For the simplicity of calculations they are not completed at this temperature but at 250°C and with all rods completely withdrawn. The increase in temperature decreases and removal of RR2 increases the multiplication factor *k*, which must be taken into account. This is done by applying the isothermal temperature coefficient and the reactivity curve of RR2 the measurements of which will be described later. Also the effects of the homogeneous model approximation must be considered when comparing the experimental results to the computational ones. With these corrections the comparable experimental value and thus the desired result of simulation becomes $k = 0.9921$ for the homogenous model and $k = 1.0011$ for the heterogeneous one. All experimental results in the following tables have been corrected to be comparable to the simulations, unless otherwise mentioned.

In the 70-fuel-subassembly core the criticality was achieved at the constant temperature of 200°C by varying the position of regulation rods. All safety rods were fully withdrawn and the criticality was achieved with regulation rods at about their half insertion. When adjusted the measured value to be comparable with the simulation, $k = 0.9897$ and $k = 0.9981$ are obtained. The experimental and computational figures of the homogeneous model are summarized in Tables 1 and the results based on the heterogeneous model are presented in Table 2. The last two columns of the tables present the relative difference between experimental and simulated results. The error margins of the simulations presented in the tables are determined by the standard deviation given by the codes and they express the statistical error only. All other sources of uncertainty have been ignored, but some of these are compensated for by the modifications of the experimental results.

Table 1: The criticality simulations. In RR positions the figure 70 cm stands for full withdrawal from the core.

Criticality simulations			*k*		Benchmark	(C-E)/E (%)	
Core	RR1 (cm)	RR2	MCNP	PSG	Measured *k*	MCNP	PSG
64	70	70	0.99223 ± 0.00026	0.99307 ± 0.00028	0.9921 ± 0.0069	0.013	0.098
70	35	31.7	0.98618 ± 0.00026	0.98672 ± 0.00027	0.9897 ± 0.0073	-0.356	-0.301

Table 2: Results of the criticality simulations based on the heterogeneous model

Criticality			*k*		Benchmark	(C-E)/E (%)	
Core	RR1 (cm)	RR2	MCNP	PSG	Measured *k*	MCNP	PSG
64	70	70	0.99246 ± 0.00022	0.99316 ± 0.00027	1.0011 ± 0.0018	-0.86	-0.79
70	35	31.7	0.99004 ± 0.00022	0.99078 ± 0.00027	0.9981 ± 0.0018	-0.81	-0.73

4.3 Rod worth

The experimental measurement of control rod worth was carried out with period method for RR1 and replacement method for other regulation and safety rods. The period method utilizes the reactor period through the so called *inhour-equation* that is not discussed more thoroughly here. In the replacement method a rod with known reactivity is inserted to compensate for the withdrawal of the rod with unknown reactivity, after which the reactivity difference is measured. The computer simulation was completed in a more straightforward way obeying the benchmark instructions such that the reactivity worth for each rod was simulated by having the rod fully inserted and the resultant multiplication factor was compared to that with all rods fully withdrawn. This kind of method would not be possible experimentally, since the excess reactivity would lead into a runaway behaviour of the reactor. The reactivity measurements considered here were performed in the 70-fuel-subassembly core.

More quantitatively, the rod worth in cents is given by

$$\mathrm{CRW} = \frac{k_1 - k_2}{k_1 k_2} \cdot \frac{1}{\beta_{\mathrm{eff}}} \cdot 100 \quad , \tag{1}$$

in which k_1 denotes the k of the core with fully withdrawn control rods, k_2 the k of the core with the specific control rod inserted and β_{eff} the fraction of delayed neutrons. For 70-fuel-subassembly the value β_{eff} = 0.0052151 was used in all measurements and simulations. Both of the simulated values of k include some statistical error whose quantity is the standard deviation (stdev). So the total error of the absolute CRW can be calculated by using the standard deviation Δk_i as follows:

$$\Delta(\mathrm{CRW}) = \frac{\Delta k_1}{k_1^2} + \frac{\Delta k_2}{k_2^2} \quad . \tag{2}$$

Table 3: The results of rod worth simulations compared to the respective measurements

Control rod worth, homogeneous model							
	k		Rod worth (in cents)		Benchmark	(C-E)/E (%)	
Rod	MCNP	PSG	MCNP	PSG	Measured RW	MCNP	PSG
Ref	1.01225	1.01376					
RR1	0.98987	0.99079	428.28 ± 9.83	438.61 ± 10.51	381.8 ± 35.5	12.17	14.88
RR2	0.99025	0.99102	420.85 ± 9.83	433.98 ± 10.50	379.4 ± 39.5	10.93	14.39
SR1	0.9891	0.98959	443.36 ± 9.84	461.92 ± 10.32	399.4 ± 44.7	11.01	15.65
SR2	0.98867	0.98984	451.80 ± 10.03	457.09 ± 10.13	403 ± 41.1	12.11	13.42
SR3	0.98978	0.99017	430.05 ± 9.83	450.65 ± 10.32	390.2 ± 43.7	10.21	15.49
SR4	0.98903	0.98939	444.74 ± 9.84	466.00 ± 9.93	395.2 ± 39.9	12.53	17.91
β_{eff} = 0.0052151							

Table 4: Rod worth simulations with the heterogeneous model. The value of β_{eff} = 0.0052151 was used also in these calculations.

Control rod worth, heterogeneous model							
	k		Rod worth		Benchmark	(C-E)/E (%)	
Rod	MCNP	PSG	MCNP	PSG	Measured RW	MCNP	PSG
Ref	1.01264	1.01301					
RR1	0.99384	0.99366	358.20 ± 8.38	368.61 ± 10.29	387.5 ± 8.14	-7.56	-4.87
RR2	0.99403	0.99431	354.51 ± 8.38	355.99 ± 10.28	385.8 ± 12.35	-8.11	-7.73
SR1	0.99365	0.99331	361.89 ± 8.19	375.33 ± 10.29	407 ± 16.28	-11.08	-7.78
SR2	0.99265	0.99322	381.33 ± 8.20	377.22 ± 10.49	410.7 ± 12.32	-7.15	-8.15
SR3	0.99367	0.99334	361.50 ± 8.39	374.83 ± 10.10	396.4 ± 15.86	-8.80	-5.44
SR4	0.99374	0.99353	360.14 ± 8.19	371.08 ± 10.68	400.3 ± 12.01	-10.03	-7.30

In order to obtain more precise information about the origins of the rod worth differences between the simulations and experiments a rough reactivity curve was simulated for both of the regulation rods. The comparison of the simulated and measured curves is, however, a little complicated. Again one of the problematic factors was the mutual interaction effect of the control rods. The problem concerning the homogeneous model was arisen by the fact that no model correction information was available for the rod worth including the interaction distortion. The simulations were performed without any corrections to eliminate the interaction effect, which means that the interacted experimental curve is the one to which the simulations should be compared.

The reactivity curves are depicted in Figures 5 – 8. It seems that the homogeneous model yields better results, but compared to each other the codes provide quite similar results. In every case the most noteworthy differences become visible when the rods are less than half inserted.

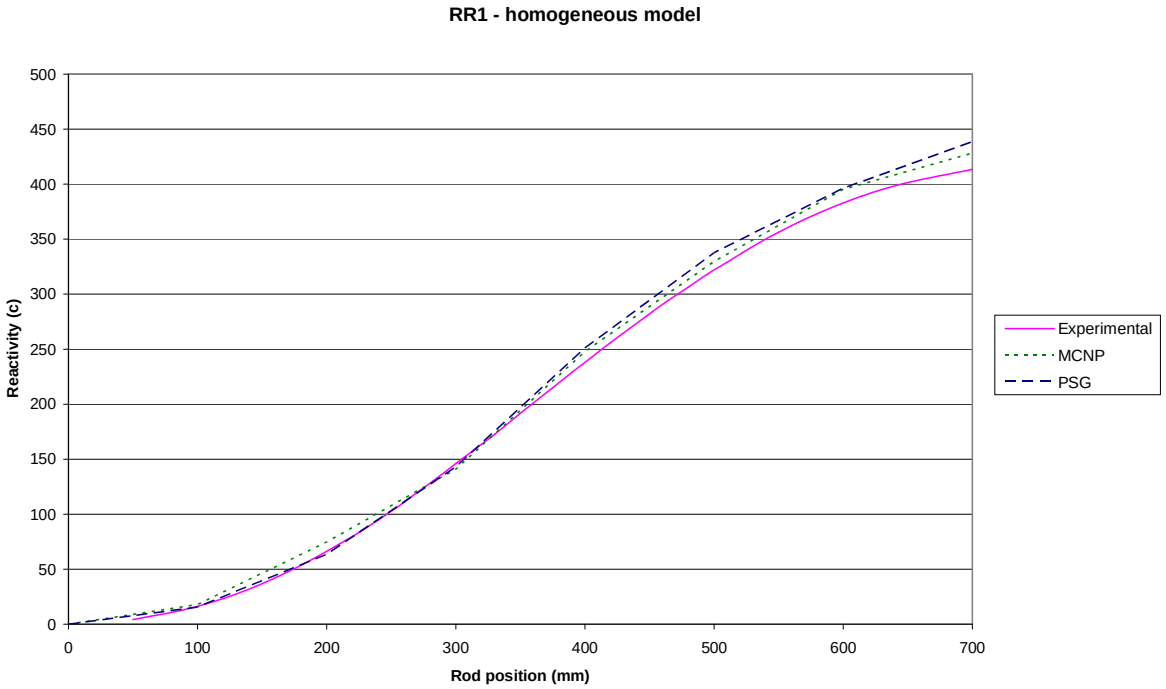

Figure 5: The reactivity curves of the regulation rod 1 produced by the homogeneous model.

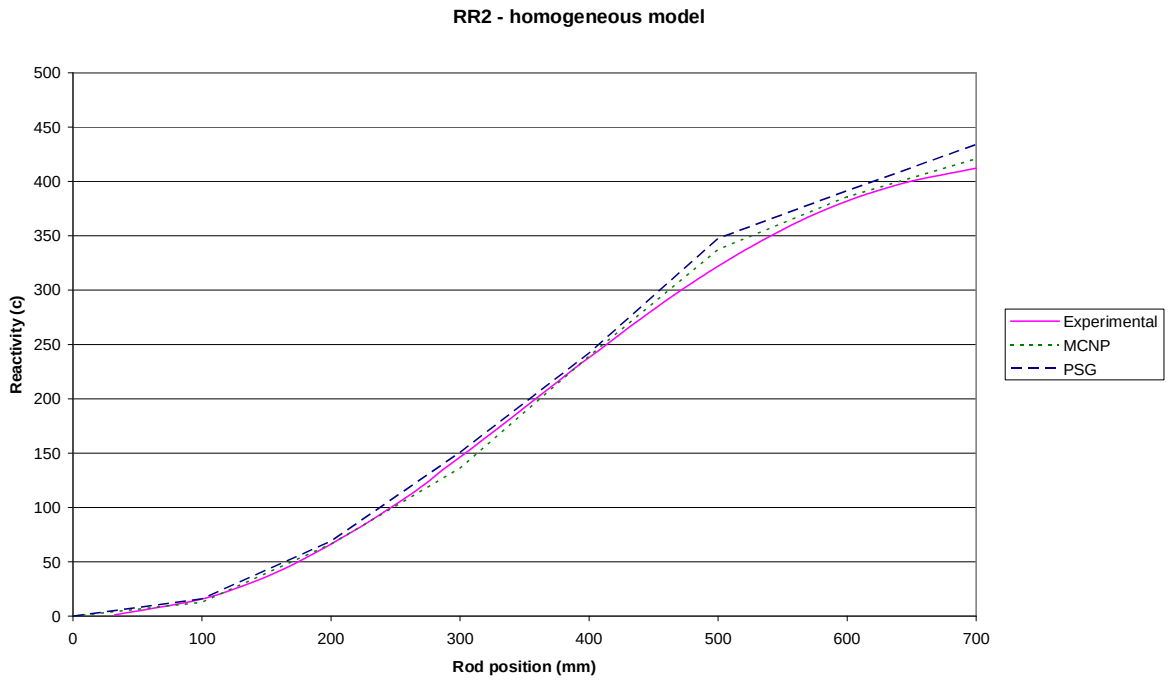

Figure 6: The reactivity curves of the regulation rod 2 when the homogeneous model was calculated.

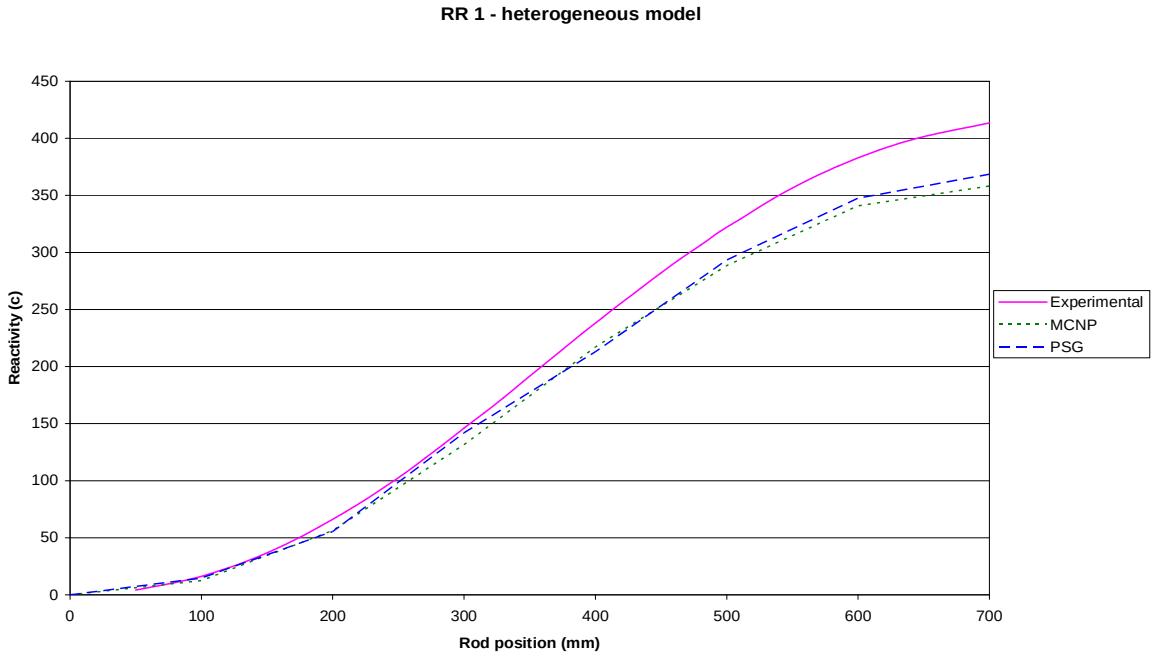

Figure 7: The simulated reactivity curves of the regulation rod 1 are quite well in line with each other, but far away from the experimentally determined curve.

Figure 8: The reactivity curves of the regulation rod 2 with heterogeneous model simulation. In this case the MCNP-simulated curve is in places surprisingly uneven, although the random error may explain some of the disruption.

4.4 Sodium void reactivity

In the real life the sodium void reactivity (SVR) was measured by replacing the sodium content of one of the fuel subassemblies by helium and comparing the resultant reactivity to the one with ordinary fuel load. The reactivity difference was obtained from the rod worth of critical core. In theory the effect of the voided volume depends on its location. To be more precise, the void tends to add reactivity in the middle of the core and diminish it near the periphery and control rods. In large reactors the void coefficient uses to be positive [3]. In order to determine the spatial dependence in JOYO the location of the voided subassembly was varied.

The position number 000 in Tables 5 and 6 means the subassembly in the middle of the core, whereas 6F1 refers to the outermost voided subassembly that is located in the blanket fuel region. The other numbers refer to the positions between the two, see Figure 1. In simulations the regulation rods were kept at 34 cm from full insertion and the safety rods were fully withdrawn. The reactivity differences were obtained from the difference of the multiplication factor between the core including a voided subassembly and the reference core. In mathematical terms this can be expressed

$$\mathrm{SVR} = \frac{k_1 - k_2}{k_1 k_2} \cdot \frac{1}{\beta_{\mathrm{eff}}} \cdot 100\,, \tag{3}$$

where k_1 represents the multiplication factor of the reference core, k_2 the k of the core with sodium removed from the specified subassembly and β_{eff} is the fraction of delayed neutrons. As in case of the control rod worth simulations the error of absolute sodium void reactivity can be calculated by using the standard deviations of the simulation:

$$\Delta(\mathrm{SVR}) = \frac{\Delta k_1}{k_1^2} + \frac{\Delta k_2}{k_2^2} \,. \qquad (4)$$

The SVR turned out to be so small that the error margins of both the simulation and experimental measurements are quite large compared to the reactivity values.

Table 5: The simulations and measurements of sodium void reactivity. It should be noted that the experimental value at the location 5F1 is not corrected to the homogeneous model but it is the direct result of the measurement.

Sodium void reactivity, homogeneous model							
Void position	*k*		SVR (in cents)		Benchmark	(C-E)/E (%)	
	MCNP	PSG	MCNP	PSG	Measured SVR	MCNP	PSG
k-ref	0.98685	0.98759					
000	0.98644	0.98752	-8.08 ± 10.44	-1.42 ± 10.15	-7.38 ± 2.51	9.62	-80.82
1F1	0.98615	0.98698	-13.79 ± 10.44	-11.92 ± 10.55	-8.12 ± 2.43	69.83	46.81
2F1	0.98594	0.98751	-17.93 ± 10.25	-1.61 ± 9.95	-8.14 ± 2.39	120.27	-80.19
3F1	0.98678	0.98717	-1.38 ± 10.63	-8.22 ± 10.15	-6.13 ± 1.98	-77.49	34.12
4F1	0.9862	0.98787	-12.81 ± 10.44	5.60 ± 10.54	-5.95 ± 2.44	115.29	-194.14
5F1	0.98674	0.98730	-2.17 ± 10.44	-5.60 ± 10.35	-2.46	-11.79	127.83
6F1	0.98724	0.98778	7.68 ± 10.23	3.66 ± 10.34	0.56 ± 1.39	1271.43	552.87
β_{eff} = 0.0052151							

Table 6: The sodium void reactivity simulations and measurements of the heterogeneous model

Sodium void reactivity, heterogeneous model							
Void position	k		Void reactivity		Benchmark	(C-E)/E (%)	
	MCNP	PSG	MCNP	PSG	Measured SVR	MCNP	PSG
k-ref	0.99123	0.99095					
000	0.99128	0.99124	0.98 ± 8.20	5.68 ± 10.54	-6.32 ± 1.87	-115.44	-189.88
1F1	0.99112	0.99064	-2.15 ± 8.20	-6.04 ± 10.74	-7.06 ± 1.76	-69.59	-14.51
2F1	0.99085	0.99052	-7.42 ± 8.20	-8.32 ± 10.74	-7.41 ± 1.87	0.12	12.31
3F1	0.99158	0.99079	6.83 ± 8.39	-3.11 ± 10.74	-5.93 ± 1.79	-215.15	-47.63
4F1	0.99119	0.99136	-0.78 ± 8.20	8.00 ± 10.93	-5.53 ± 1.9	-85.88	-244.71
5F1	0.99142	0.99092	3.71 ± 8.39	-0.53 ± 10.74	-2.46	-250.70	-78.57
6F1	0.99133	0.99130	1.95 ± 8.20	6.87 ± 10.74	0.58 ± 1.39	236.45	1084.66

4.5 Isothermal temperature coefficient

The isothermal temperature coefficient (ITC) was measured at low power by changing the reactor temperature in between 170 and 250°C. The coefficient was measured for cores with both 65 and 70 fuel subassemblies, but the simulation was calculated only for the 65-core. In the homogeneous model the measured ITC was -0.781±0.047 c/°C and the simulated one -0.685±0.126 c/°C by MCNP and -0.513±0.136 by PSG, see Table 7. The simulation results of the heterogeneous model were clearly closer to the measured value, especially when MCNP was used. These results appear in Table 8.

This is the coefficient whose negativity would be the most important for the reactor safety. According to the simulation results the negativity seems to be guaranteed, although the error margins resulting only from the statistical error are pretty wide. The simulation accuracy was further

deteriorated by the fact that a cross-section library didn't exist for the material at 250°C but the data applied was valid for 600 K (that is 327°C).

Table 7: The simulated and experimental values of isothermal temperature coefficient.

Isothermal temperature coefficient, homogeneous model							
	k		ITC (in cents)		Benchmark	(C-E)/E (%)	
Temp	MCNP	PSG	MCNP	PSG	Measured ITC	MCNP	PSG
170	0.99198	0.99138					
250	0.98915	0.98926	-0.685 ± 0.126	-0.513 ± 0.136	-0.781 ± 0.047	-12.25	-34.32
β_{eff} = 0.0052605							

Table 8: The isothermal temperature coefficients resulting from the heterogeneous model.

Isothermal temperature coefficient, heterogeneous model							
	k		ITC		Benchmark	(C-E)/E (%)	
Temp	MCNP	PSG	MCNP	PSG	Measured ITC	MCNP	PSG
170	0.99348	0.99418					
250	0.9904	0.99048	-0.744 ± 0.106	-0.893 ± 0.140	-0.769 ± 0.022	-3.28	16.10

5 CONCLUSIONS

Both the homogeneous and heterogeneous models simulated by MCNP and PSG provided results some of which were quite well in line with the experimental ones and others not so much. Especially the simulations of the sodium void reactivity illustrated the feature of the Monte Carlo method that its accuracy is strictly limited. Most of the experimental results were within the simulated void coefficient error margins, but it gives no valuable information on the sign of the coefficient. According to the observation it doesn't pay off to research small reactivity changes by using Monte Carlo codes. Much more computer power or time would be needed. However, even a ten-fold initial neutron population would not diminish the statistical error sufficiently.

The simulations concerning the rod worth of the control rods showed that the codes result in quite similar values. It is outstandingly interesting that the simulations of the homogeneous model seemed to be more realistic and the curves were smoother than the ones with the heterogeneous model. The study of the rod reactivities was disturbed by the rod interaction effect, which was taken into account in the experimental work but ignored in simulations. The comparison between the simulated and measured reactivity curves was possible since the non-corrected experimental results were available for the regulation rods. This information lacked for the safety rods, which caused a problem when comparing the total rod worth measurements and simulations. For more information some simulations should be performed to determine the computational interaction coefficient.

The simulation uncertainties presented with the results were the statistical errors provided by the codes and they didn't take into account any other error sources caused by physical factors. For example the cross-section data was not available exactly for the right temperature. The distortion was systematically present in all simulations, but the isothermal temperature coefficient simulation was the only one that included essential temperature dependence. The ITC simulations also suffered from a pretty large statistical error thanks to which all simulations and measured values overlapped except for the PSG simulation with the homogeneous model.

The best match between the simulated and measured results was obtained in criticality simulations where they were separated by fractions of percents only. Also in this case the homogeneous model simulation results were closer to the experimental ones than the results of heterogeneous model simulations. An explanation for the better congruence may be the fact that the

criticality was the only research subject in which the examined results were not based on a difference of two multiplication factors.

ACKNOWLEDGEMENTS

This work was part of the NETNUC project funded by the Academy of Finland and VTT.

REFERENCES

[1] "Japan's Experimental Fast Reactor JOYO MK-I -core: Sodium-cooled Uranium-Plutonium Mixed Oxide Fueled Fast Core surrounded by UO2 Blanket", International Handbook of Evaluated Reactor Physics Benchmark Experiments, NEA/NSC/DOC(2006)1. OECD/NEA, 2006.

[2] J. Leppänen: "Development of a New Monte Carlo Reactor Physics Code", Doctoral Thesis, 2007

[3] B. Lundell: "Snabba bridreaktorer", Studsvik Report, 1991 (in Swedish)